厚生労働科学研究費補助金

認知症対策総合研究事業

細胞を血行性脳実質内動員する機序の解析およびそのアルツハイマー病治療への応用に関する研究

平成21年度　総括研究報告書

研究代表者　内村　健治

平成22(2010)年　3月

別紙2

目　　次

別紙3

厚生労働科学研究費補助金（認知症対策総合研究事業）
総括研究報告書

細胞を血行性脳実質内動員する機序の解析および そのアルツハイマー病治療への応用に関する研究

研究代表者　　内村　健治　　独立行政法人　国立長寿医療研究センター　室長

研究要旨：　本研究はアルツハイマー病の病態に伴って骨髄単球由来ミクログリア細胞が脳内へ移行性を示すという知見をもとに、細胞の血行性脳実質内動員の分子メカニズムを明らかにすることを目的とする。また、脳移行性細胞をアルツハイマー病治療における遺伝子の脳内搬送体として利用する細胞医薬への応用を目指す。昨年度までに本研究者はマウスミクログリア細胞株BV2が細胞表面分子セレクチンリガンド糖鎖シアリルルイスXを発現すること、加齢アルツハイマー病モデルマウス脳血管においてセレクチンが発現誘導されることを明らかにした。さらに、脳血管内での末梢投与ミクログリア細胞の動態を生体内ビデオ蛍光顕微鏡によりライブイメージング解析する技術を確立した。我々は本年度、当該解析方法により加齢アルツハイマー病モデルマウス脳血管内におけるBV2のローリングおよび強固な接着を確認した。これらの頻度が野生型マウスに比べて有意に増加する知見が得られた。セレクチンは炎症時における炎症細胞の組織内浸潤に重要である。我々はリポ多糖（LPS）で全身性に炎症状態を呈するマウスの脳血管でも加齢アルツハイマー病モデルマウス脳で観られたローリングおよび強固な接着の増加を観察した。アルツハイマー病態脳における骨髄単球由来ミクログリアの脳移行性にはセレクチンとその糖鎖リガンドの分子相互作用が重要である事が強く示唆され、そのメカニズムは炎症におけるメカニズムと一部共通する可能性が示された。一方、我々は細胞医薬により脳内へ送り込む遺伝子の候補としてAD病理変化を低減させると思われるヘパラン硫酸糖鎖細胞外スルファターゼSulfを明らかにした(Hossain et al., Glycobiology, 2010)。ポリオーマウィルスベクターを用いると脳移行ミクログリア細胞において効率よく外来遺伝子を発現させ得ることを確認した。これらの結果はアルツハイマー病態を軽減させる遺伝子の脳内搬送および発現システムの基盤技術に繋がる成果と期待された。

A．研究目的

骨髄単球由来ミクログリアがアルツハイマー病の病態に伴い脳内に浸潤することが報告されている（Simard et al., Neuron, 2006; El Khoury et al., Nat Med 2007など）。脳内へ移行した細胞はアルツハイマー病発症の物質的基盤であるアミロイド沈着体を貪食能などにより積極的に除去する働きを示すものと考えられている。これらの細胞は、動脈投与または静脈投与により血行性に脳内へ浸潤・生着する。詳細なメカニズムは未だ不明である。アルツハイマー病を含む神経変性疾患の治療法は、血液脳関門の存在などにより大きく制限されている。本研究は単球由来ミクログリア、アルツハイマー病モデルマウスおよび生体内ビデオ蛍光顕微鏡法を用いて当該細胞の脳血管外遊走と脳内への移入メカニズムを明らかにすることを目的とする。アミロイド斑分解除去遺伝子の脳内搬送体としてこれら細胞を利用する細胞医薬をもとにしたアルツハイマー病の新しい治療法開発の技術

基盤の提供も目指す。

B．研究方法

本研究者は白血球の血管から標的末梢組織内へ浸潤する際の分子機序を以前明らかにした（Uchimura et al., Nature immunol 2005、Veerman et al., Nature Immunol 2007など）。具体的には、セレクチンとそのリガンド糖鎖の分子相互作用が血管内白血球ローリングに重要であることを明らかにした。本研究ではこの末梢組織細胞浸潤解析において確立した生体内ビデオ蛍光顕微鏡法を脳内細胞浸潤解析に応用し未だ不明な脳血管外遊走と脳内移行機序を個体レベルで解析した。セレクチンリガンド糖鎖を発現するマウスミクログリア細胞株（BV2）およびセレクチンを脳血管内で発現する加齢アルツハイマー病モデルマウスを使用した。代謝ラベル法によりBV２をCFSE蛍光色素標識し、11-12ヶ月齢のアルツハイマー病モデルマウスTg2576の脳内における動態をThin-skull法および生体内ビデオ蛍光顕微鏡を用いて解析した。コントロールとして同じ月齢のNon-Tgマウスを用いた。2ヶ月齢の野生型マウスにLPS(15g/mouse)を腹腔内投与し4時間経過後、CFSE標識したBV2(4×10^6)を尾静脈より投与した。同様に脳内における動態を観察した。外来遺伝子の発現システム構築にはマウスミクログリア細胞株（MG5）を用いた。培養MG5にZsGreen蛍光タンパク質遺伝子を組み込んだ各種ウィルスベクター(1×10^8 particles)を感染させ60時間後にZsGreen陽性細胞数を測定した。本センター研究所 中西章室長の研究協力により実施した。

一方、福祉村病院長寿医学研究所 赤津裕康副所長の研究協力によりヒトアルツハイマー病患者剖検脳におけるセレクチンおよび多硫酸化ヘパラン硫酸糖鎖ドメインの発現解析を実施した。

（倫理面への配慮）

研究実施に先立ち、各研究実施協力機関の倫理委員会による厳正中立な審査を受け、研究実施計画の承認を受ける。特にヒト試料を用いた研究実施に際しては人権の保護および個人情報の保護に最大限の注意を払うことを理解遵守し一層の徹底を図る。また、1）インフォームドコンセントの徹底、2）検体の使用及び保存についての中止請求を含む研究協力同意書の十分な説明、3）検体保存責任者を設置し当該者以外には連結不可能な匿名化を施したうえでのサンプル及びデータの保管、さらにスタンドアローンのコンピューターを用いたデータ処理、鍵のかかるキャビネット内へのデータ保管を行う。 本研究において遺伝子の抽出・保管および遺伝子発現の解析は行わず、遺伝情報に触れる事はない。

研究実施に先立ち、研究実施機関である国立長寿医療センターの倫理委員会による厳正中立な審査を受け、研究実施計画の承認を受けた。本申請研究で実施するモデルマウス対象研究はすべて本センター設置の遺伝子組換え生物実験安全委員会の審査を受け承認を得た。また、本センター設置の実験動物委員会および動物実験倫理委員会の審査を受け承認を得た。本研究課題に参画する者は「遺伝子組換え生物等の使用等の規制による生物の多様性の確保に関する法律（カルタヘナ法）」、「動物の愛護及び管理に関する法律」および「動物を用いる生物医学研究のための国際指導原則」の更なる理解を確認し遵守した。

C．研究結果

生体内ビデオ蛍光顕微鏡解析により加齢アルツハイマー病モデルマウス脳血管内におけるBV2のローリングおよび強固な接着を確認した。これらの頻度が野生型マウスに比べて有意に増加する知見が得られた。セレクチンは炎症時における炎症細胞の組織内浸潤に重要である。LPS感作マウスにおいてBV2細胞の脳血管内腔における解析

を行った結果、BV2のローリングおよび接着の増加が観察された。加齢Tg2576アルツハイマー病モデルマウスの脳血管内解析結果とほぼ同じことが観察された。MG5感染実験の結果、マウスポリオーマウィルスPY2スベクターを用いた時、選択的に90%以上の細胞に外来遺伝子を発現させることが確認された。サルポリオーマウィルスSV40, JC1, JC2ヒトポリオーマウィルスJC, BK, 向Bリンパ球パポーバウィルスLPV2, LPV2REP, サルパポーバウィルスSA12, マウス向肺ウィルスKiham、いずれのベクターも30%以上の細胞発現効率を示さなかった。また、脳内へ送り込む遺伝子の候補としてAD病理変化を低減させると思われるヘパラン硫酸糖鎖細胞外スルファターゼSulfを明らかにした(Hossain et al., Glycobiology, 2010)。ヒトアルツハイマー病剖検脳側頭葉におけるセレクチン分子の発現上昇をウェスタンブロット法により一部明らかにした。ヒトサンプルの採取はすべて医療法人さわらび会福祉村病院で行ったものを用いた。ヒトサンプルの解析はすべて国立長寿医療センター 研究所で行った。

D．考察

マウスミクログリア細胞株BV2がアルツハイマー病モデルマウス脳血管内において野生型では観られないローリングおよび接着の増加を示すことが示された。さらに、LPS感作による全身性炎症マウスでも同様に観察された。これらの事から，細胞のアルツハイマー病態脳内浸潤メカニズムは炎症におけるメカニズムと一部共通する可能性が示された。BV2はL-セレクチン分子やPSGL-1(P-セレクチンリガンド分子)は発現しないがE-セレクチンリガンド分子（シアリルルイスX糖鎖）は発現する。BV2の脳内血管におけるローリングの増加はE-セレクチンとそのリガンド分子を介した相互作用による結果であることが示唆された。脳移行性ミクログリアを外来遺伝子脳内搬送体として利用する事を検討するためこれらの細胞に効率良く遺伝子を導入発現させるシステムの開発を検討した。マウスポリオーマウィルスPY2スベクターの選択的な高効率遺伝子発現結果はこのベクターを用いたシステム構築が有用であることを示している。ヒトアルツハイマー病剖検脳側頭葉におけるセレクチン分子の発現上昇結果はアルツハイマー病の大部分を占める孤発性アルツハイマー病の発症メカニズム解析へマウスの知見が応用できることを強く示唆することとなった。

E．結論

アルツハイマー病の病態に伴って骨髄単球由来ミクログリア細胞が脳内へ移行性を示す際の分子メカニズムがセレクチンとそのリガンド糖鎖を中心に解明された。また、炎症時に働くメカニズムと共通な作用が存在する事が示唆された。脳移行性細胞にポリオーマウィルスPY2ベクターを用いて遺伝子を脳内搬送させる細胞医薬の技術基盤の提供が今後期待される。本研究で得られたADモデル動物における知見および結果を今後スケール拡大したヒト臨床サンプルの使用による臨床研究へ発展させることが強く望まれた。

F.健康危険情報

該当なし。

G．研究発表

１．論文発表

Hossain MM, Hosono-Fukao T, Tang R, Sugaya N, van Kuppevelt TH, Jenniskens GJ, Kimata K, Rosen SD, Uchimura K. Direct detection of HSulf-1 and HSulf-2 activities on extracellular heparan sulfate and their inhibition by PI-88. Glycobiology. 20:175-86. (2010)

２．学会発表

細野友美，モタラブ　ホサイン，マーカスブリッチギ、道川 誠 ，トインクッペヴェルト、トニーワイスコレイ、 内村健治
ヘパラン硫酸多硫酸化ドメインのアルツハイマー病モデルマウス脳内における発現解析
第73回日本生化学中部支部例会・シンポジウム、名古屋、平成２１年５月２３日

内村健治
細胞の血行性組織内浸潤に関わる細胞表面セレクチンリガンド糖鎖-リンパ球ホーミング，骨髄細胞アルツハイマー病脳内浸潤-
信州大学大学院医学研究科講義、2009年6月1日、松本

細野友美、ホサインモタラブ、Britschgi M，赤津裕康、道川誠、van Kuppevelt T，Wyss-Coray T，内村健治
アルツハイマー病態脳におけるヘパラン硫酸糖鎖の解析
第３回GFRG研究会　８月２５日，北海道大学

細野友美、ホサインモタラブ、マーカスブリッチギ、赤津裕康、道川誠、トインクッペヴェルト、トニーワイスコレイ、内村健治
アルツハイマー病態脳におけるヘパラン硫酸鎖内部ドメインの発現解析
第２９回日本糖質学会年会、高山市、平成２１年９月１０日

ホサインモタラブ、細野友美、レンホンタン、高之瀬邦子、道川誠、トインクッペヴェルト、スティーブローゼン、内村健治
ヘパラン硫酸多硫酸化ドメインの脳内における発現解析およびSulfによる分解
第２９回日本糖質学会年会、高山市、平成２１年９月１１日

細野友美、マーカスブリチギ，赤津裕康、道川誠、トインクッペベルト，トニーワイスコレイ，内村健治
アルツハイマー病脳アミロイド沈着におけるRB4CD12抗体認識ヘパラン硫酸鎖内部ドメインの蓄積
第82回日本生化学会大会　神戸国際会議場，2009年10月24日，神戸.

ホサインモタラブ、細野友美、レンホンタン，道川誠、トインクッペベルト，スティーブンローゼン，内村健治
RB4CD12抗体が認識する細胞外スルファターゼ修飾ヘパラン硫酸内部ドメインのマウス脳内における発現
第82回日本生化学会大会　神戸国際会議場，2009年10月24日，神戸.

Tomomi Hosono, Motarab Hossain, Markus Britschgi, Hiroyasu Akatsu, Makoto Michikawa, Tony Wyss-Coray, Kenji Uchimura
Highly sulfated domains of heparan sulfate accumulate in cerebral Aß plaques
Society for Neuroscience meeting, Chicago, 10/21/2009. Chicago

Kenji Uchimura
Sulfated endothelial ligands involved in cell migration into lymph nodes
IMMAG Seminar, Medical College of Georgia, 10/15/2009, Augusta

細野友美，ホサインモタラブ，マーカスブリチギ，赤津裕康、道川誠、トニーワイスコレイ，内村健治
Highly sulfated domains of heparan sulfate accumulate in amyloid plaques of Alzheimer's disease brain
グローバルCOE第2回国際シンポジウム　名古屋ヒルトンホテル　2009年11月27日，名古屋

ホサインモタラブ,細野友美,高之瀬邦子,道川誠,スティーブンローゼン,内村健治
Cerebral immunolocalization of the RB4CD12 anti-heparan sulfate epitope and its degradation by Sulfs, extracellular endosulfatases
グローバルCOE第2回国際シンポジウム　名古屋ヒルトンホテル　2009年11月27日，名古屋

細野友美,ホサインモタラブ,マーカスブリチギ，赤津裕康、道川誠,トインクッペヴェルト,トニーワイスコレイ，内村健治
アルツハイマー病態脳におけるヘパラン硫酸糖鎖多硫酸化ドメインの発現解析
第28回日本認知症学会　東北大学百周年記念会館，　2009年11月20日,仙台.

Tomomi Hosono, Motarab Hossain, Markus Britschgi, Hiroyasu Akatsu, Makoto Michikawa, Tony Wyss-Coray, Kenji Uchimura
Highly sulfated domains of heparan sulfate accumulate in cerebral Aß plaques of patients and mouse models of Alzheimer's disease
第2回Nagoyaグローバルリトリート　愛知健康プラザ　2010年2月26日，大府

H. 知的財産権の出願・登録状況（予定を含む。）
１．特許取得
なし

２．実用新案登録
なし

３．その他
なし

別紙４

研究成果の刊行に関する一覧表

雑誌

発表者氏名	論文タイトル名	発表誌名	巻号	ページ	出版年
Hossain MM, Hosono-Fukao T, Tang R, Sugaya N, van Kuppevelt TH, Jenniskens GJ, Kimata K, Rosen SD, Uchimura K.	Direct detection of HSulf-1 and HSulf-2 activities on extracellular heparan sulfate and their inhibition by PI-88.	Glycobiology	20	175-186	2010

研究成果の刊行物・別刷

Glycobiology vol. 20 no. 2 pp. 175–186, 2010
doi:10.1093/glycob/cwp159
Advance Access publication on October 12, 2009

Direct detection of HSulf-1 and HSulf-2 activities on extracellular heparan sulfate and their inhibition by PI-88

Md Motarab Hossain[3], Tomomi Hosono-Fukao[3], Renhong Tang[4], Noriko Sugaya[5], Toin H van Kuppevelt[6], Guido J Jenniskens[2,6], Koji Kimata[5], Steven D Rosen[4], and Kenji Uchimura[1,3,4]

[3]Section of Pathophysiology and Neurobiology, National Institute for Longevity Sciences, 36-3 Gengo, Morioka, Obu, Aichi 474-8522, Japan; [4]Department of Anatomy, Program in Immunology, University of California, San Francisco, CA, USA; [5]Research Complex for the Medicine Frontiers, Aichi Medical University, Japan; and [6]Department of Biochemistry 280, Nijmegen Centre for Molecular Life Sciences, Radboud University Nijmegen Medical Center, The Netherlands

Received on February 8, 2009; revised on September 30, 2009; accepted on September 30, 2009

Heparan sulfates (HS) bind a diversity of protein ligands on the cell surface and in the extracellular matrix and thus can modulate cell signaling. The state of sulfation in glucosamines and uronic acids within the chains strongly influences their binding. We have previously cloned and characterized two human extracellular endoglucosamine 6-sulfatases, HSulf-1 and HSulf-2, which selectively liberate the 6-*O* sulfate groups on glucosamines present in *N*, 6-*O*, and 2-*O* trisulfated disaccharides of intact HS and heparins. These enzymes serve important roles in development and are upregulated in a number of cancers. To determine whether the Sulfs act on the trisulfated disaccharides that exist on the cell surface, we expressed HSulfs in cultured cells and performed a flow cytometric analysis with the RB4CD12, an anti-HS antibody that recognizes *N*- and *O*-sulfated HS saccharides. The endogenously expressed level of the cell surface RB4CD12 epitope was greatly diminished in CHO, HEK293, and HeLa cells transfected with HSulf-1 or HSulf-2 cDNA. In correspondence with the RB4CD12 finding, the *N*, 6-*O*, and 2-*O* trisulfated disaccharides of the HS isolated from the cell surface/extracellular matrix were dramatically reduced in the Sulf-expressed HEK293 cells. We then developed an ELISA and confirmed that the RB4CD12 epitope in immobilized heparin was degraded by purified recombinant HSulf-1 and HSulf-2, and conditioned medium (CM) of MCF-7 breast carcinoma cells, which contain a native form of HSulf-2. Furthermore, HSulf-1 and HSulf-2 exerted activity against the epitope expressed on microvessels of mouse brains. Both HSulf activities were potently inhibited by PI-88, a sulfated heparin mimetic with anti-cancer activities. These findings provide new strategies for monitoring the extracellular remodeling of HS by Sulfs during normal and pathophysiological processes.

[1]To whom correspondence should be addressed: Tel: +81-562-46-2311; Fax: +81-562-46-3157; e-mail: arumihcu@nils.go.jp
[2]Present address: ModiQuest Research BV, Nijmegen, Netherlands.

Keywords: confocal microscopy/extracellular sulfatase/flow cytometry/heparan sulfate/PI-88

Introduction

Heparan sulfate proteoglycans (HSPGs) are cell surface or extracellular matrix components, which consist of core protein to which one or more glycosaminoglycan chains are covalently attached (Bernfield et al. 1999; Esko and Lindahl 2001). Heparan sulfate (HS) chains and heparins (structural analogs of HS chains) comprise repeating disaccharide units of glucuronic/iduronic acid (GlcA/IdoA) and glucosamine (GlcN) that are modified through a set of deacetylation, epimerization, and sulfation reactions (Gallagher 2001). The *N*-, 3-*O*, and 6-*O* positions of glucosamine and the 2-*O* position of the uronic acid residues in the HS disaccharide units are potentially substituted by sulfate groups by a group of Golgi-resident HS sulfotransferases (Habuchi et al. 2004). These synthetic reactions along the HS chains are spatially and temporally regulated, conferring upon the chains structural diversity, which underlie important roles in pathological and biological processes (Lin 2004; Parish 2006; Bishop et al. 2007). HS contain highly sulfated domains, "S-domains," and partially sulfated or non-sulfated domains, which are transitional (Gallagher 2001; Powell et al. 2004). S-Domains are the most common units in heparin. Within the S-domains, a trisulfated disaccharide structure [-IdoA(2-OSO_3)-$GlcNSO_3$(6-OSO_3)-] occurs. This structure is considered to be a key element in molecular interactions between HS/heparin and many protein ligands, including growth factors and chemokines (Esko and Selleck 2002; Kreuger et al. 2006). We have previously identified and cloned a human extracellular endosulfatase (HSulf-1), an ortholog of QSulf-1 (Dhoot et al. 2001). We also described a closely related protein, designated HSulf-2 (Morimoto-Tomita et al. 2002). Both Sulfs are posttranslationally modified with *N*-linked glycans (Morimoto-Tomita et al. 2002; Ambasta et al. 2007) and formylglycines (Cosma et al. 2003; Dierks et al. 2003), processed by furin endoproteases and can be secreted (Morimoto-Tomita et al. 2002; Tang and Rosen 2009). The Sulfs remove 6-*O* sulfates on glucosamine residues in the trisulfated disaccharides of heparin (Morimoto-Tomita et al. 2002; Saad et al. 2005) and heparan sulfate (Ai et al. 2003; Viviano et al. 2004). Sulf-2 mobilizes heparin-bound vascular endothelial growth factor (VEGF), FGF-1, and SDF-1 (Uchimura et al. 2006a). The enzyme is proangiogenic in the chick chorioallantoic membrane assay, presumably through its ability to reverse the association between angiogenic factors and heparin/HSPGs (Morimoto-Tomita et al. 2005). Studies of quail and Xenopus embryos (Dhoot et al. 2001; Freeman et al. 2008) and of Sulf-deficient mice have demonstrated developmental roles for the Sulfs (Lamanna et al. 2006; Ai et al. 2007; Holst

et al. 2007; Lum et al. 2007). Furthermore, increasing evidence implicates the Sulfs in cancer, in some cases augmenting cancer cell growth and in others inhibiting it (Lai et al. 2004, 2008; Dai et al. 2005; Narita et al. 2007; Nawroth et al. 2007).

Antibodies against HS have been established as useful tools to evaluate the expression and localization of HS in cultures and tissues. The 10E4 monoclonal anti-heparan sulfate antibody (David et al. 1992) has been widely used to detect HS in biological and pathological sets. Another monoclonal anti-heparan sulfate antibody, HepSS-1, has also been characterized (van den Born et al. 2005). The HS epitopes of recently developed phage display antibodies have been defined using derivatives of HS and heparins (van Kuppevelt et al. 1998). One of them, RB4CD12, recognizes *N*- and *O*-sulfated saccharides of HS/heparin (Jenniskens et al. 2000; Dennissen et al. 2002). Its recognition epitope is proposed to be [-GlcNSO$_3$(6-OSO$_3$)-IdoA(2-OSO$_3$)-GlcNSO$_3$(6-OSO$_3$)-], a trisulfated disaccharide-containing HS oligosaccharide (Jenniskens et al. 2002). In the present study, we have employed RB4CD12 to demonstrate that HSulfs exhibit 6-*O*-endoglucosamine activities against HS on the cell surface of transfected cells and in the extracellular matrix (ECM) of mouse brain microvessels, as well as on immobilized heparin in an ELISA. We then use RB4CD12 to show that both Sulfs are potently inhibited by PI-88, an antiangiogenic and antimetastatic agent.

Results

Cell surface expression of the RB4CD12 epitope is diminished by transfection of HSulf cDNA

RB4CD12 is a single-chain variable fragment (scFv) antibody selected for reactivity to skeletal muscle heparin/HS glycosaminoglycans utilizing a phage display system (Jenniskens et al. 2000). RB4CD12 recognizes highly sulfated HS/heparin saccharide structures present in S-domains of HS and heparin. Antibody binding depends on all three sulfate modifications (Dennissen et al. 2002). The 10E4 mAb is widely used as a reporter for HS expression in cells and tissues. The 10E4 epitope is known to involve HS oligosaccharides that contain GlcNSO$_3$ and GlcNAc residues with *O*-sulfations dispensable (van den Born et al. 2005). We found by flow cytometry that the RB4CD12 and 10E4 epitopes were expressed on the cell surface of wild-type CHO cells (Figure 1A). To confirm that the RB4CD12 epitope on CHO cells was dependent on HS structures and not on chondroitin sulfate (CS), we employed mutant CHO cells in which the biosynthesis of glycosaminoglycans was disrupted. The pgsA-745 cell line is deficient in both HS and CS synthesis (Esko et al. 1985). The pgsD-677 cell line is HS deficient but CS sufficient. Staining with RB4CD12 antibody was not observed in either pgsA-745 or pgsD-677 cells (Figure 1A) but was present in wild-type cells (Jenniskens et al. 2000). 10E4 staining of these cells showed the same pattern (Figure 1A).

As reviewed above, HSulf-1 and HSulf-2 remove 6-*O*-sulfates from heparin/HS chains (Morimoto-Tomita et al. 2002; Ai et al. 2003; Viviano et al. 2004). Analysis of HS chains in cells derived from Sulf null mice is also consistent with this enzyme specificity (Lamanna et al. 2006, 2008; Ai et al. 2007). To determine whether the cell surface expression level of the sulfated saccharide structure was reduced by the HSulfs, we established CHO cells stably transfected with cDNA encoding HSulf-1 or

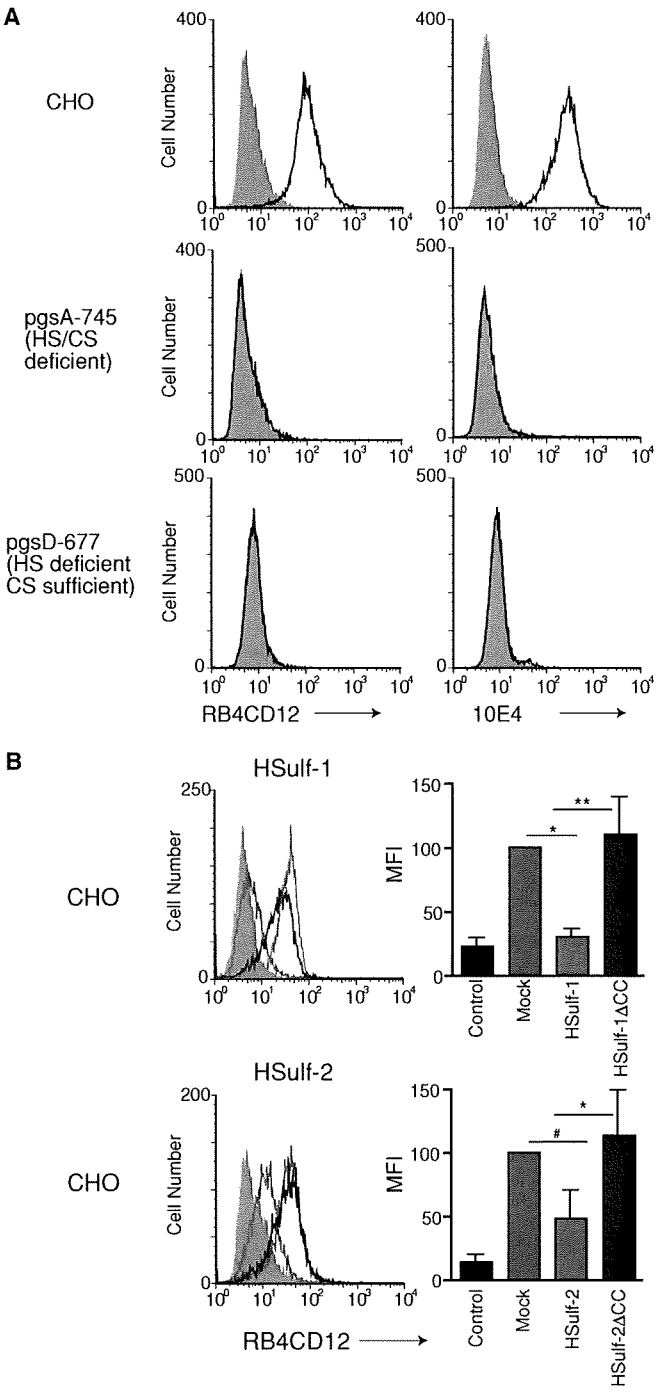

Fig. 1. Cell surface expression of the RB4CD12 heparan sulfate epitope in wild-type, heparan sulfate-deficient, and HSulf-transfected CHO cells. (**A**) Wild-type CHO cells (CHO), CHO deficient in glycosaminoglycan xylosylation initiation (pgsA-745), or CHO deficient in heparan sulfate chain polymerization (pgsD-677) were analyzed by flow cytometry with RB4CD12 scFv or 10E4. (**B**) Flow cytometry of CHO cells stably transfected with pcDNA3.1 empty vector alone (Mock); cDNA of HSulf-1 (HSulf-1), HSulf-1ΔCC (HSulf-1ΔCC), HSulf-2 (HSulf-2), or HSulf-2ΔCC (HSulf-2ΔCC) were analyzed for staining with RB4CD12. These data are representative of three independent determinations. Mean fluorescence intensity (MFI) relative to "Mock" of three independent determinations is shown. MPB49, a non-HS binding scFv antibody, was used as "control". **, $P < 0.001$; *, $P < 0.01$; #, $P < 0.05$.

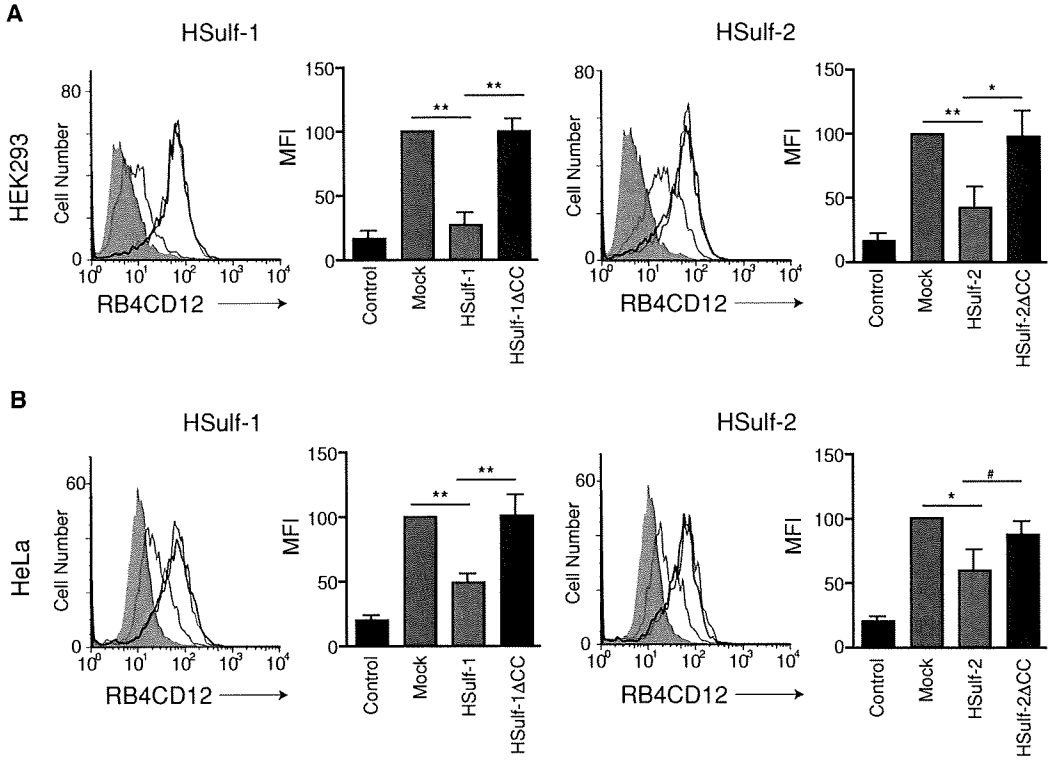

Fig. 2. Cell surface expression of the RB4CD12 epitope in HSulf-transfected HEK293 and HeLa cells. HEK293 (**A**) and HeLa (**B**) cells transiently transfected with a pcDNA3.1 empty vector alone (Mock); cDNA of HSulf-1 (HSulf-1), HSulf-1ΔCC (HSulf-1ΔCC), HSulf-2 (HSulf-2), or HSulf-2ΔCC (HSulf-2ΔCC) were analyzed by flow cytometry with RB4CD12. These data are representative of at least three independent experiments. Mean fluorescence intensity (MFI) relative to "Mock" of three independent experiments is shown. MPB49, a non-HS binding scFv antibody, was used as "control". **, $P < 0.001$; *, $P < 0.01$; #, $P < 0.05$.

HSulf-2 and performed flow cytometry with RB4CD12. A non-HS control staining (MPB49 antibody) was employed to show the basal level of the staining signal. HSulf-1 diminished the cell surface expression to 25% of the level seen in the unaffected mock control, as quantified by mean fluorescence intensity (MFI) (Figure 1B). HSulf-2 reduced expression to 50% of the background level (Figure 1B). CHO cells expressing inactive forms of enzymes (HSulf-1ΔCC and HSulf-2ΔCC) retained RB4CD12 staining equivalent to that of the mock transfectant (Figure 1B). We also examined the effects of the Sulfs on the expression of the RB4CD12 epitope in transiently transfected HEK 293 and HeLa cells. Transfection with either HSulf-1 or HSulf-2 cDNA significantly reduced the RB4CD12 epitope on the surface of these cells (to 25% in HEK293 with HSulf-1, 40% in HEK293 with HSulf-2, 50% in HeLa with HSulf-1, 60% in HeLa with HSulf-2), consistent with the results obtained with CHO stable transfectants (Figure 2A and B). Cells transfected with HSulf-1ΔCC or HSulf-2ΔCC plasmids sustained the epitope at the control level (Figure 2A and B). We also stained Sulf-transfected HEK293 and HeLa cells with the HepSS-1 antibody (van den Born et al. 2005). HSulf-1 expression significantly augmented staining with the antibody in HEK293 (3.2-fold) and HeLa cells (1.2-fold) (Supplementary Figure 1A). HSulf-2 increased the level of HepSS-1 staining on both cell types (1.5-fold in HEK293, 1.2-fold in HeLa cells) (Supplementary Figure 1B). Expression of inactive forms of HSulf-1 and HSulf-2 (HSulf-1ΔCC and HSulf-2ΔCC) did not alter staining by HepSS-1 (Supplementary Figure 1A and B). We examined the

Table I. Disaccharide composition of extracellular HS of HSulf-transfected HEK 293 cells. Total extracellular HS was degraded with a mixture of heparinases I, II, and III. The products were subjected to reverse-phase ion pair chromatography with a post-column fluorescent labeling. The values are representative of two independent experiments

	Unsaturated disaccharide[a]						
Transfectant	ΔDi-0S	ΔDi-NS	ΔDi-6S	ΔDi-(N,6)diS	ΔDi-(N,2)diS	ΔDi-(N,6,2)triS	Total 6-*O*-sulfation[b]
Mock	49.7 (100)	14.5 (100)	13.5 (100)	9.1 (100)	9.2 (100)	3.9 (100)	26.5 (100)
HSulf-1	55.1 (110.7)	15.8 (109.1)	14.3 (105.7)	4.8 (52.8)	9.2 (100.3)	0.8 (19.2)	19.8 (74.7)
HSulf-1 ΔCC	50.9 (102.3)	14.5 (100)	13.4 (99.5)	9.3 (102.3)	7.8 (84.2)	4.1 (104.2)	26.8 (101.1)
Hsulf-2	51.6 (103.6)	15.7 (108.2)	14.0 (103.4)	6.9 (75.4)	10.2 (111.1)	1.6 (42.1)	22.5 (84.9)
HSulf-2 ΔCC	49.5 (99.6)	15.2 (104.9)	13.5 (99.9)	9.2 (101.4)	7.7 (83.5)	4.8 (123.2)	27.5 (103.8)

[a]Percentage of total disaccharides (% of "Mock").
[b]Percentage of total 6-*O*-sulfation (% of "Mock") determined by the sum of the percentages of 6-*O*-sulfated disaccharide products.

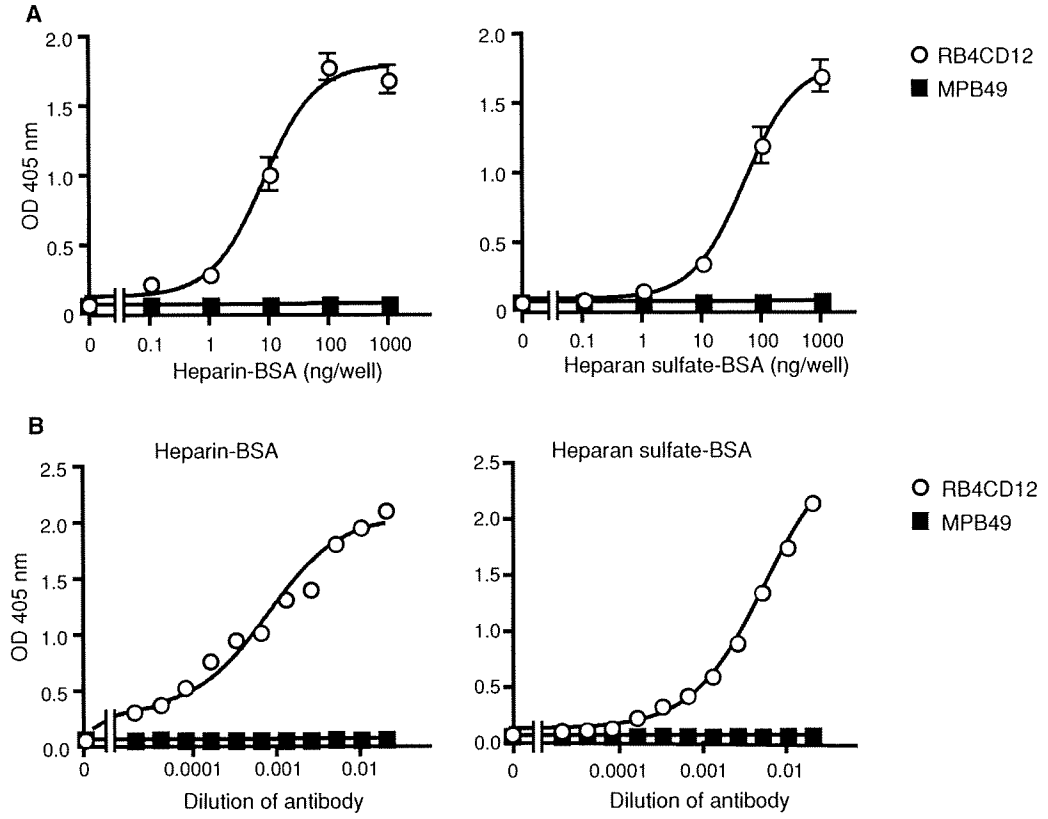

Fig. 3. ELISA for the RB4CD12 epitope with immobilized heparin and heparan sulfate. (**A**) RB4CD12 was tested for binding to varying amounts of immobilized heparin-BSA or heparan sulfate-BSA by ELISA. (**B**) Reaction of serially diluted RB4CD12 to immobilized heparin-BSA (10 ng/well) or heparan sulfate-BSA (100 ng/well). MPB49 is a non-HS binding phage display antibody used as a control. Data in (**B**) are representative of two independent trials.

structure of HS isolated from the cell surface/ECM of Sulf-transfected HEK293 cells. The disaccharide composition of the isolated HS was analyzed. Transfection with either HSulf-1 or HSulf-2 cDNA substantially reduced the trisulfated disaccharide units of the HS (to 19% and 42% of the "Mock" control level with HSulf-1 and HSulf-2, respectively) (Table I). A moderate reduction was observed in total 6-*O*-sulfation of the isolated HS (to 75% and 85% of the "Mock" control level with HSulf-1 and HSulf-2, respectively) (Table I).

The RB4CD12 epitope on heparin is degraded by recombinant HSulfs

We then asked whether HSulf-1 and HSulf-2 could reduce the RB4CD12 epitope in a cell-free ELISA. The RB4CD12 antibody recognized heparin-BSA (>1 ng/well) and heparan sulfate-BSA (>10 ng/well) immobilized onto plastic wells (Figure 3A) in a concentration-dependent manner (Figure 3B). Amino terminal FLAG-tagged, carboxy terminal His-tagged HSulf-1 and HSulf-2, and corresponding inactive mutants (HSulf-1ΔCC and HSulf-2ΔCC) were purified from the conditioned medium (CM) of transfected HEK293 cells on Ni-NTA beads (Figure 4A). Immunoblotting with an anti-FLAG antibody revealed two specific protein bands in HSulf-1 and HSulf-1ΔCC (~135 and ~75 kDa) and three specific bands in HSulf-2 and HSulf-2ΔCC (~240, ~135, and ~75 kDa) (Figure 4A). It has recently been reported that the 75 kD, ~135 kD, and ~240 kD bands correspond to the N-terminal subunit, the heterodimer of N- and C-terminal subunits, and a higher order oligomer, respectively (Tang and Rosen 2009). RB4CD12 binding to heparin-BSA was substantially reduced by pre-treatment of the heparin-BSA with the purified HSulf-1 (reduced to 45% of control) or HSulf-2 (reduced to 35% of control), (Figure 4B). HSulf-1ΔCC and HSulf-2ΔCC had only minor effects on RB4CD12 binding. The effects of the inactive Sulfs in the RB4CD12 assays might be attributable to a competing heparin-binding activity of Sulf protein due to its basic hydrophilic domain (Morimoto-Tomita et al. 2002; Ai et al. 2006; Frese et al. 2009). A mixture of heparinases was used as a positive control for digestion of immobilized heparin and was found to reduce the RB4CD12 recognition by >90% (Figure 4B). Both HSulf-1 and HSulf-2 reduced binding of RB4CD12 to heparin-BSA in a time-dependent manner (Figure 4C).

The RB4CD12 epitope on heparin is degraded by MCF-7 conditioned medium

We have previously shown that MCF-7 cells, a human breast carcinoma cell line, produce Sulf-2 and secretes the protein into CM as an active form (Morimoto-Tomita et al. 2005; Uchimura et al. 2006a). To determine if a native form of Sulf exhibited the same activity as the recombinant enzyme, we employed the MCF-7 CM. Pretreatment of immobilized heparin-BSA with a fixed concentration of MCF-7 CM produced a >80% reduction in RB4CD12 binding (Figure 5A). The activity was both concentration- and time-dependent (Figure 5B and C). After centrifugation of MCF-7 CM at 100,000 × *g* for 1 h, HSulf-2 protein was detected in both the supernatant and the

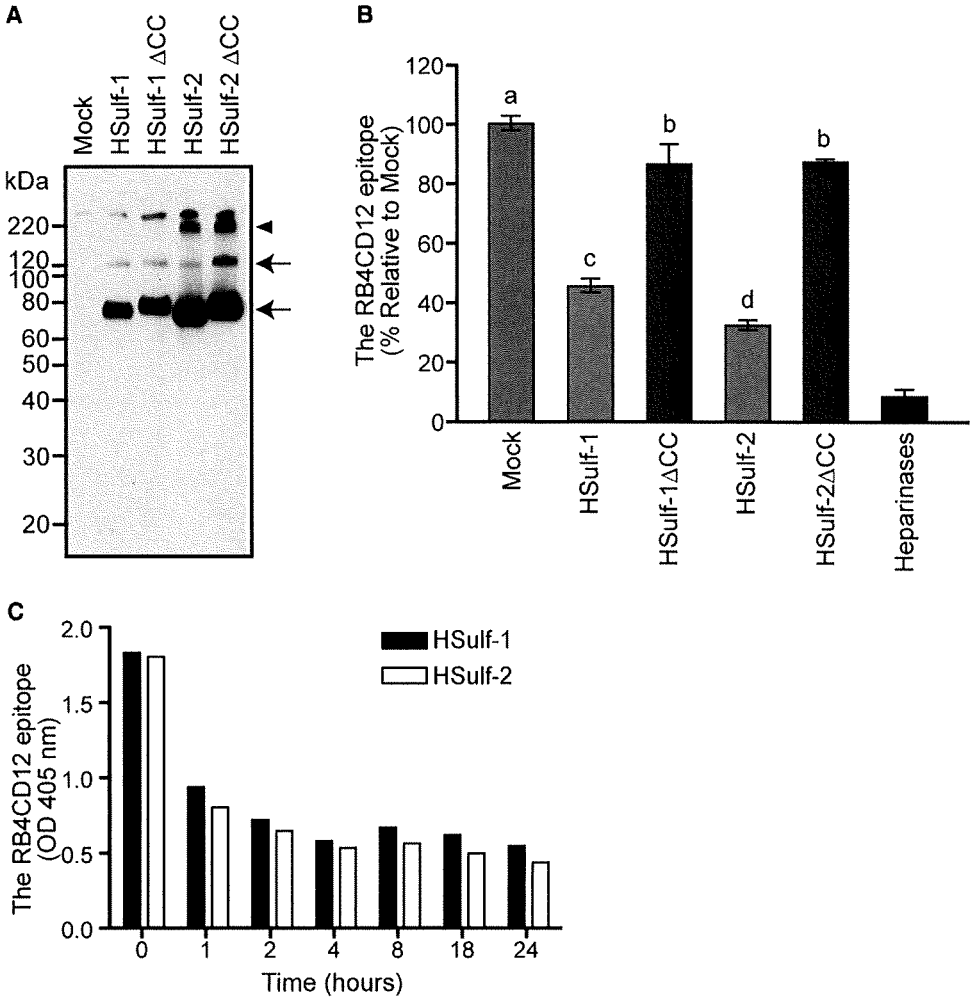

Fig. 4. Expression of recombinant HSulf-1 and HSulf-2 and their effects on the RB4CD12 epitope in immobilized heparin. (**A**) Recombinant HSulfs (HSulf-1 and HSulf-2) and their enzymatically inactive forms (HSulf-1ΔCC and HSulf-2ΔCC) tagged with N-terminal FLAG and C-terminal His were produced in HEK293 cells. The proteins were purified on Ni-NTA beads and subjected to immunoblotting for the FLAG tag. The "Mock" control was based on testing bead-bound materials from vector control transfected HEK293 cells. Specific bands detected in HSulf-1 and HSulf-1ΔCC (~130 and ~75 kDa, arrows) and in HSulf-2 and HSulf-2ΔCC (~240, ~130 and ~75 kDa, arrows and an arrowhead) are denoted. Note that a slight shift of bands in HSulf-1ΔCC and HSulf-2ΔCC was also seen in our previous work (Uchimura et al. 2006a). (**B**) The purified Sulfs were tested for their effects on immobilized heparin-BSA in the RB4CD12 epitope ELISA. The Sulfs were prepared from 0.5 mL of CM collected from the transfected HEK293 cells. A mixture of bacterial heparinases I, II, and III was used as a control for the epitope degradation (heparinases). Different letters among treatments indicate significant differences ($P < 0.05$). (**C**) The Sulfs purified from 0.5 mL of the CM were tested as a function of reaction time in the RB4CD12 ELISA.

precipitate (Figure 5D). Both fractions exhibited activity (Figure 5D). By scanning the blot in Figure 5D, the Sulf activities relative to HSulf-2 proteins in both fractions were determined. The specific activities in the supernatant and the precipitate were comparable (data not shown). Preclearing the CM with the H2.3 anti-HSulf2 antibody reduced the activity to 55%, while control IgG did not, confirming that the reduction in RB4CD12 binding was due to HSulf-2 (Figure 5E). Thus, a significant portion of secreted Sulf-2 meets a stringent test of solubility and retains its enzymatic activity.

HSulfs degrade the RB4CD12 epitope in tissue

To determine whether the HSulfs could degrade the RB4CD12 epitope in tissues, we treated cryostat-cut sections of mouse brains with HSulfs. RB4CD12 stained microvessels in sections of mouse brain (Figure 6A). The staining co-localized with laminin, a marker of basement membranes (Figure 6A). No specific staining was observed when RB4CD12 substituted with MPB49 (data not shown). Treatment of sections with purified HSulf-1, purified HSulf-2, or MCF-7 CM produced significant reductions in RB4CD12 staining of microvessels. Similarly, treatment with heparinases also diminished staining. For quantification, the intensity of RB4CD12 staining was normalized to that of laminin (see Material and methods). HSulf-1 and HSulf-2 reduced RB4CD12 staining to 70% and 65%, respectively, of the "Mock" treatments (Figure 6B). MCF-7 CM and a mix of heparinases reduced RB4CD12 staining to 52% and 35%, respectively, of the "no enzyme" treatments (Figure 6B).

PI-88 inhibits the Sulfs

PI-88 is a phosphomannopentaose polysulfate, which was developed as an inhibitor of heparanase, an endoglycosidase which

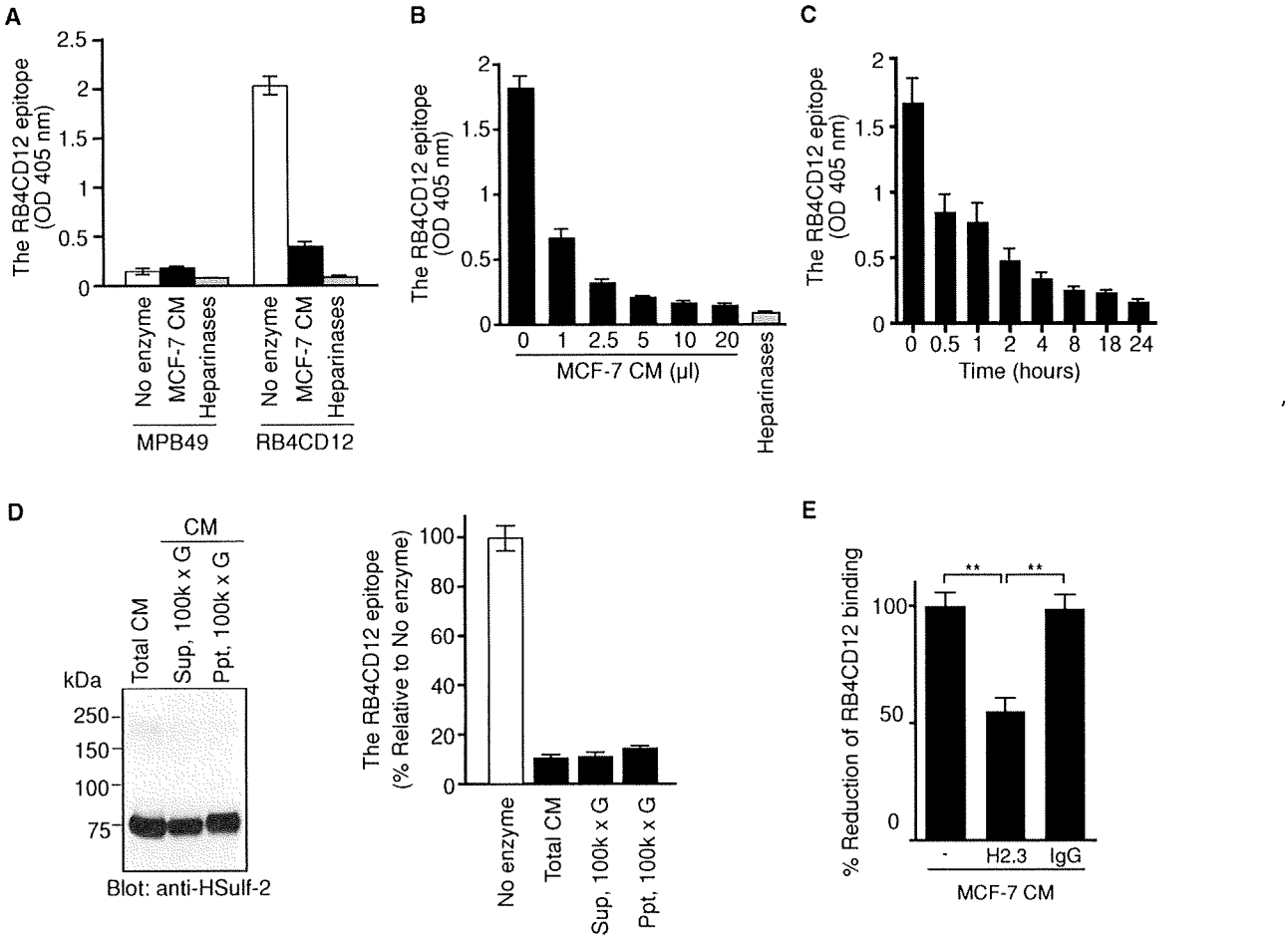

Fig. 5. The effect of MCF-7 conditioned medium (CM) on the RB4CD12 epitope in heparin. (**A**) The effect of MCF-7 conditioned medium (10 µL, overnight incubation time) on the RB4CD12 epitope in immobilized heparin-BSA. (**B** and **C**) The activity of MCF-7 CM on the RB4CD12 epitope as a function of CM volume (1 h incubation) and reaction time (1 µL of CM). MPB49, a non-HS binding scFv antibody, was used as a control for RB4CD12. A mixture of bacterial heparinases I, II, and III was used as a positive control to produce epitope degradation (heparinases). (**D**) HSulf-2 was analyzed by immunoblotting in unfractionated MCF-7 CM (5 µg protein, "total CM"), the supernatant fraction (5 µg protein, "Sup, 100 k × *g*") and the precipitated fraction (1.5 µg protein, "Ppt, 100 k × *g*") of the CM after a centrifugation at 100,000 × *g* for 1 h. HSulf-2 protein was detected by H2.3 anti-HSulf2 antibody (Morimoto-Tomita et al. 2005). The activity of each fraction (with the same amount of proteins as above) was analyzed by the RB4CD12 ELISA (overnight incubation). (**E**) Inhibition of the activity in MCF-7 CM by the H2.3 anti-HSulf2 antibody. Two micrograms of H2.3 antibody or rabbit IgG was incubated with MCF-7 CM (1 µL, 4 h incubation). **, $P < 0.001$.

cleaves HS chains (Khachigian and Parish 2004). Since PI-88 was designed as a heparin mimetic, we wanted to know whether it might inhibit the Sulfs. We first tested its activity in the heparin-BSA ELISA described above. Reduction of the RB4CD12 epitope produced by HSulf-1, HSulf-2 (Figure 7A), or MCF-7 CM (Figure 7B) was efficiently inhibited by PI-88 in a dose-dependent manner. We previously showed that treatment of heparin-BSA with MCF-7 CM reduced the subsequent binding of $VEGF_{165}$ (Uchimura et al. 2006a). When PI-88 was mixed with MCF-7 CM, its inhibitory activity in this assay was blunted (Figure 7C). IC50 and LogIC50 values of PI-88 in these various assays are summarized in Table II.

Table II. Effects of PI-88 on Sulf activities

Enzyme	Analyzed effect[a]	IC50[b] (µg/mL)	LogIC50[c]
HSulf-1	Degradation of RB4CD12 epitope	2.6	2.5 ± 0.1
HSulf-2	Degradation of RB4CD12 epitope	1.2	0.9 ± 0.1
MCF-7 CM	Degradation of RB4CD12 epitope	0.6	0.9 ± 0.2
	Pre-binding effect on $VEGF_{165}$	3.6	2.9 ± 0.1

[a]These effects were measured and shown in Figure 7.
[b]The concentration of PI-88 that inhibited the Sulf enzymatic activity by 50%.
[c]Means ± SE.

Discussion

A large body of evidence has established that the Sulfs can modulate the signaling activities of a variety of HS-binding factors (Wnts, FGFs, noggin, HGF, GDNF) during development (Ai et al. 2003, 2007; Viviano et al. 2004; Freeman et al. 2008) and tumor growth (Lai et al. 2004; Dai et al. 2005; Nawroth et al. 2007). Besides these establishments, a more direct approach for the detection of the glucosamine-6-endosulfatase activities of the Sulfs has been anticipated. Here using a phage display-derived antibody, RB4CD12, we have devised a general method, compatible with both flow cytometry and immunohistochemistry, to monitor the actions of Sulf-1 and Sulf-2 on the

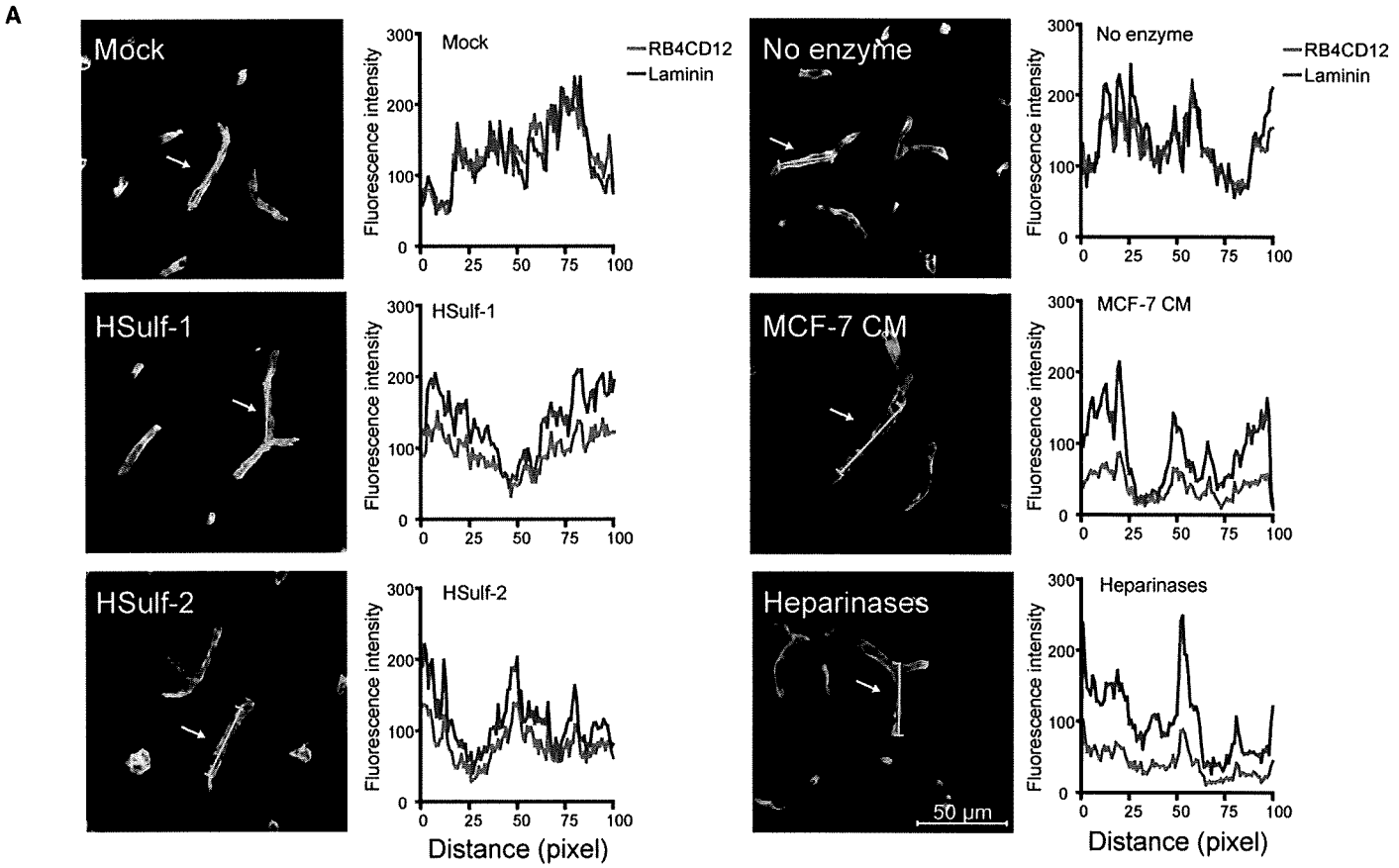

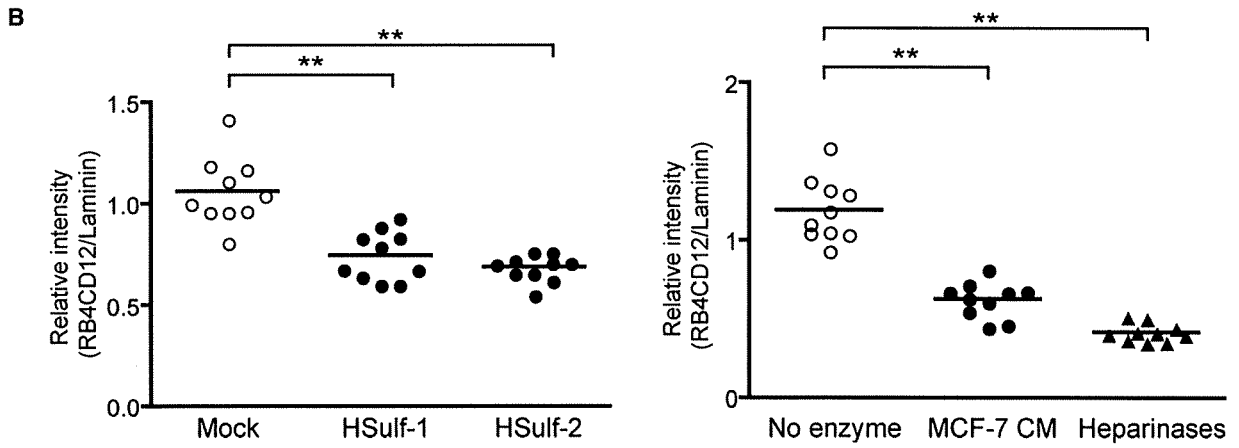

Fig. 6. Sulf degradation of the RB4CD12 epitope in the basement membrane of mouse brain microvessels. (**A**) Cryostat-cut sections of mouse brains were incubated overnight with recombinant HSulf-1 (0.4 µg) and HSulf-2 (0.4 µg) prepared from CM of transfected HEK293 cells (HSulf-1, HSulf-2), buffer only (no enzyme), or CM of MCF-7 human breast cancer cells (MCF-7 CM). The Ni-NTA resin-bound materials that were prepared from HEK293 cells transfected with the empty vector were eluted and used (Mock). A mix of bacterial heparinases (Heparinases) served as a positive control. RB4CD12 binding was visualized by a Cy3-conjugated anti-VSV tag antibody with a confocal laser scanning microscopy (red). Basement membranes of vessels were stained by an anti-laminin antibody in conjunction with a Cy2-conjugated secondary antibody (green). The signal intensities along the line markers (blue lines) indicated by *arrows* in the images were measured for RB4CD12 and laminin staining as described in *Material and methods*. Representative images and measurements of 10 randomly selected vessels are shown. (**B**) The relative intensity of RB4CD12 to laminin is shown, $n = 10$ vessels per treatment. Data are from two experiments with five vessels analyzed in distinct brain specimens from two donors for each treatment. Each symbol represents one vessel image; small horizontal lines indicate the mean. Magnification used 630×. **, $P < 0.001$.

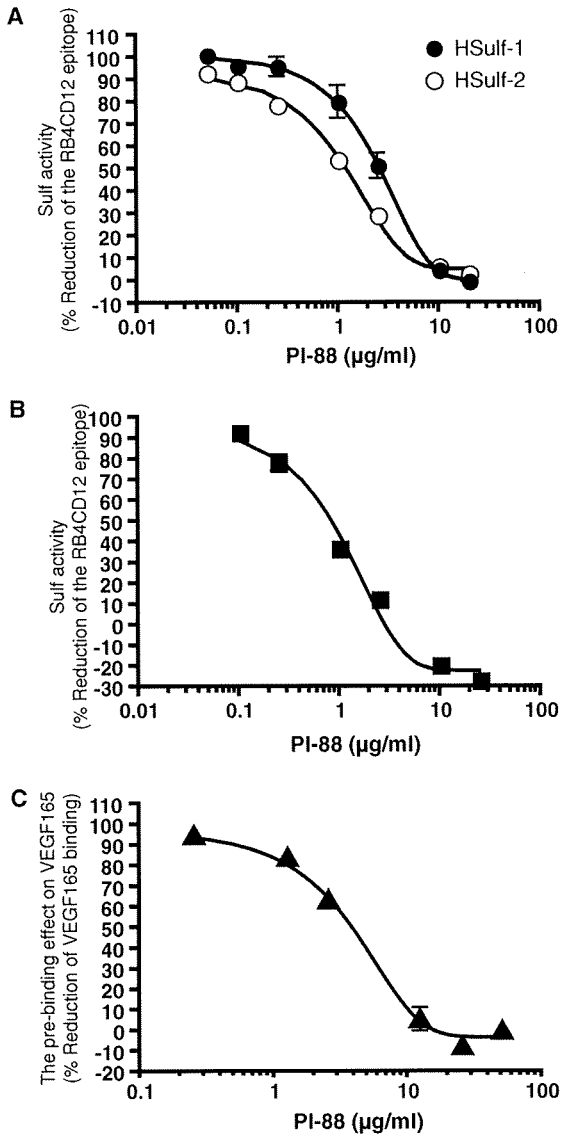

Fig. 7. Inhibition of HSulf-1 and HSulf-2 activities by PI-88. Purified recombinant Sulfs (HSulf-1, 0.4 μg and HSulf-2, 0.4 μg) (**A**) and MCF-7 CM (10 μL) were used (**B**). PI-88 was tested at varying concentrations for its ability to inhibit the action of the Sulfs and the CM on the RB4CD12 epitope of immobilized heparin by ELISA as described in *Material and methods*. (**C**) PI-88 at varying concentrations was tested for its ability to inhibit the action of MCF-7 CM (10 μL) to reduce the binding of $VEGF_{165}$ to immobilized heparin-BSA in a solid phase binding assay (Uchimura et al. 2006a). PI-88 exhibited negligible activity when assays were performed without the CM (data not shown). Over the concentration of 0.1 μg/mL (both HSulf-1 and HSulf-2) (**A**), 0.25 μg/mL (MCF-7 CM) (**B**), and 1.25 μg/mL (MCF-7 CM) (**C**), the data are statistically significant ($P < 0.05$). The values were analyzed by one-way ANOVA with Dunnett's test against the value obtained without PI-88.

cell surface and the ECM. RB4CD12 recognizes highly sulfated domains within HS since it reacts with highly sulfated oligosaccharides with most likely dependence on the presence of 6-*O*-, *N*-, and 2-*O*- sulfate esters (Dennissen et al. 2002). The antibody prefers oligosaccharides containing both $GlcNSO_3(6\text{-}OSO_3)$ and $IdoA(2\text{-}OSO_3)$ (Dennissen et al. 2002; Jenniskens et al. 2002). As predicted from the specificity of the antibody, stable (CHO) or transient (HEK293, HeLa) transfection of Sulfs reduced the cell surface expression of the RB4CD12 epitope. The reduction in the *N*-, 6-*O*-, and 2-*O*- trisulfated disaccharide units [-$IdoA(2\text{-}OSO_3)$-$GlcNSO_3(6\text{-}OSO_3)$-] (by 58–81%) observed in cell surface/ECM HS of HSulf-transfected cells is consistent with the reduction of the RB4CD12 epitope at the cell surface. The moderate loss (15–25%) of overall HS 6-*O*-sulfation in the HS of HSulf-transfected cells suggested that RB4CD12 specifically recognizes the trisulfated disaccharide structure as a component of the HS oligosaccharide [-$GlcNSO_3(6\text{-}OSO_3)$-$IdoA(2\text{-}OSO_3)$-$GlcNSO_3(6\text{-}OSO_3)$-]. The expected parallel increase in *N*- and 2-*O*-disulfated disaccharide units in cell surface/ECM HS of HSulf-transfected cells was not observed. The basis for this result remains to be explained. We found that Sulf transfection generally caused a moderate increase in cell surface staining by HepSS-1. The increase in staining may reflect newly formed product via the enzymatic action of the HSulfs. Another possibility is that the accessibility of the antibody to the epitope was increased by liberation of 6-*O*-sulfate groups from HS chains.

It was possible that the effects we observed on the RB4CD12 epitope of transfected cells were due to primary action of the Sulfs but secondary signaling responses in the cells. We therefore carried experiments on heparin in a cell-free setting. The trisulfated disaccharide unit is a major structural unit (~80% of total disaccharide units) in heparin. To show direct effects of the Sulfs on the RB4CD12 epitope, we established a solid-phase ELISA employing immobilized heparin as a substrate. As seen in Figure 4C, both HSulf-1 and HSulf-2 diminished the epitope in immobilized heparin at a saturation level by 70–75% binding, consistent with our previous demonstration that the Sulfs can degrade 80% of the total trisulfated disaccharide units in soluble heparins (Morimoto-Tomita et al. 2002). In the same ELISA, MCF-7 CM also exhibited strong degradation of the RB4CD12 epitope (by ~80%) (Figure 5). The activity of the CM against the RB4CD12 epitope in immobilized heparin proceeded linearly up to 8 h. We attribute this activity to Sulf-2, as we have shown the specific inhibition of the activity by the H2.3 anti-HSulf2 antibody and have previously demonstrated that the endoglucosamine-6-sulfatase activity of MCF-7 CM resides in native Sulf-2 (Uchimura et al. 2006a). The Sulf activity and the HSulf-2 protein in MCF-7 CM were detected in both the supernatant and the precipitate after a centrifugation at 100,000 × *g*. The precipitate fraction contains the most of extracellular membrane vesicle components (Kim et al. 2002). Our data suggest that HSulf-2 might be able to associate with extracellular membrane vesicles, such as exosomes (Thery et al. 2002). We found that recombinant and native Sulfs reduced the RB4CD12 epitope on the basement membrane of brain microvessels. The degree of activity of the Sulfs could possibly be reflected by their enzyme stability and/or post-translational modifications (Zito et al. 2005). Besides verifying the activity of Sulfs on HS in a tissue context, this finding suggests the possible utility of this antibody as an immunohistochemical reporter of Sulf activity in situ.

PI-88 inhibits metastasis and angiogenesis during the growth and progression of solid tumors and is currently in clinical trials for several cancers. (Parish et al. 1999; Joyce et al. 2005). PI-88 may act through its inhibition of heparanase, an enzyme implicated in the remodeling of extracellular matrix by cancer cells (Joyce et al. 2005; Ilan et al. 2006; Vlodavsky et al. 2007). However, PI-88 also blocks a number of growth factor–HS

interactions and may interfere with the signaling activities of these factors. We found that PI-88 also inhibited the Sulfs with IC50s in the range of 0.6–3.6 μg/mL (Table II), which are comparable to that for heparanase (2 μg/mL) (Parish et al. 1999). For several cancers, significant subsets of patients show upregulation of Sulf transcripts in tumors (Iacobuzio-Donahue et al. 2003; Li et al. 2005; Morimoto-Tomita et al. 2005; Nawroth et al. 2007; Lai et al. 2008). Furthermore, Sulf-2 is proangiogenic and can promote the growth of cancer cells in vitro and in vivo (Nawroth et al. 2007; Lai et al. 2008). Thus, the inhibitory effects of PI-88 on tumor progression might be attributable, at least in part, to inactivation of the Sulfs. The development of more selective Sulfs inhibitors should allow testing of this possibility. The assays described herein may provide the basis for screening chemical libraries for further examples of Sulf inhibitors.

Material and methods

Materials

The following materials were obtained commercially from the source indicated. Heparin conjugated with bovine serum albumin (Heparin-BSA), heparinases (I, II and III), monoclonal anti-VSV (vesicular stomatitis virus) glycoprotein-Cy3™ antibody, and monoclonal anti-FLAG® antibody were from Sigma (St. Louis, MO); CHO wild-type (CHO-K1), CHO mutants (pgsA-745, pgsD-677), and HeLa cells were from ATCC (Manassas, VA); HEK293 and MCF-7 cells were from Japan Health Science Research Resources Bank (Osaka, Japan); polyclonal rabbit anti-VSV-G antibody was from Bethyl Laboratories (Montgomery, TX); Cy™3-conjugated goat anti-Mouse IgM μ chain, alkaline phosphatase-conjugated polyclonal goat anti-rabbit IgG (H+L) and Cy™2-conjugated goat anti-Rabbit IgG (H+L) were from Jackson Immuno Research Laboratories (West Grove, PA); recombinant human VEGF-165 and polyclonal goat anti-human VEGF antibody were from R&D Systems (Minneapolis, MN); a biotinylated swine anti-goat IgG (H+L) antibody, a streptavidin conjugated with alkaline phosphatase, horseradish peroxidase-conjugated goat anti-mouse IgG1 antibody were from Caltag Laboratories (Burlingame, CA); 10E4 and HepSS-1 monoclonal anti-heparan sulfate antibodies were from Seikagaku (Tokyo, Japan). The RB4CD12 phage display-derived anti-heparan sulfate antibody (also known as HS3A8) was produced in a VSV-tag version and purified as described previously (Dennissen et al. 2002). DEAE-Sepharose™ was from GE Healthcare UK Ltd (Buckinghamshire, England). Heparan sulfate conjugated with BSA was prepared as described previously (Uchimura et al. 2006a). PI-88 (Parish et al. 1999) was provided by Progen Pharmaceutics Ltd.

Cell culture and transfection

CHO cells were cultured in Ham's F12 medium containing 10% fetal bovine serum (FBS) at 37°C in 5% CO_2. HEK293 and HeLa cells were cultured in Dulbecco's Modified Eagle Medium containing 10% FBS. CHO, HEK293, and HeLa cells were transfected with pcDNA3.1 Myc/His-HSulf1, -HSulf2, -HSulf1ΔCC or -HSulf2ΔCC expression plasmid (Morimoto-Tomita et al. 2002) using the FuGENE® 6 transfection reagent according to the manufacturer's instructions (Roche Diagnostics, Basel, Switzerland). HSulf-1ΔCC and HSulf-2ΔCC are enzymatically inactive with two cysteines mutated to alanines (Morimoto-Tomita et al. 2002). Stable CHO transfectants were selected with 1 mg/mL G418 (Invitrogen). In transient transfections, the transfection efficiency was measured by counting the percentage of green-fluorescent cells in parallel experiments with an expression plasmid encoding green fluorescent protein. The efficiency was determined to be ~60% in HEK293 and HeLa cells.

Preparation of HSulfs

N-terminal-FLAG-, C-terminal-His-tagged versions of HSulf1, HSulf2, HSulf1ΔCC, or HSulf2ΔCC in the pSecTag plasmid (Uchimura et al. 2006a) were prepared. HEK293 cells were transiently transfected with FuGENE® 6 and then grown in OptiMEM (Invitrogen) at 37°C in 5% CO_2 for 48 h. Ten milliliters of conditioned medium (CM) was collected and mixed with 100 μL of a Ni-NTA agarose resin (Pro-Bond™ resin, Invitrogen) followed by rotation at 4°C for 4 h. After incorporation into a chromatography column (Poly-Prep® column, Bio-Rad), the resin was washed with the buffer containing 50 mM HEPES, pH 7.5, and 0.05% Tween 20 (20 times the volume of the resin). The resin-bound proteins were eluted with the buffer containing 50 mM HEPES, pH 7.5, 10 mM $MgCl_2$, and 100 mM imidazole (double volume of the resin). The "Mock" control was prepared from CM of HEK293 cells transfected with an empty vector. Native HSulf-2 was obtained from CM of cultured MCF-7 cells, a human breast carcinoma cell line (Morimoto-Tomita et al. 2005). The cells were grown in RPMI-1640 containing 10% FBS in a 150 cm^2 flask. Cells (80% confluent) were rinsed with phosphate-buffered saline (PBS) and OptiMEM, and then incubated in 25 mL of OptiMEM at 37°C in 5% CO_2 for 72 h. The CM was collected and then 100-fold concentrated on a Centricon-30 (Millipore). Subsequently, the concentrated CM was dialyzed into 50 mM HEPES, pH 7.5. The CM was fractionated into a supernatant (soluble fraction) and a precipitate (containing membrane fragments) by centrifugation (100,000 × *g* for 1 h at 4°C). The supernatant was 100-fold concentrated as above. The precipitate was dissolved in the buffer containing 50 mM HEPES, pH 7.5, and 0.05% Tween-20.

Cell surface expression of heparan sulfate epitopes

Adherent cells were detached from culture flasks by incubating in 0.02% EDTA/PBS (Sigma) at 37°C for 10 min and then dissociated into monodispersed cells. Cells (1×10^5) were collected and suspended in 100 μL 1× FACS buffer (1% BSA and 0.1% NaN_3 in PBS, filtered by a 0.22 μm filter unit) containing an Fc Blocker (eBioscience) and incubated at 4°C for 15 min. Then, 10E4 (10 μg/mL), HepSS-1 (20 μg/mL), or RB4CD12 (1:50 dilution) were added to the suspension. Parallel staining was also done with mouse IgM (eBioscience, San Diego, CA), as isotype-matched control for 10E4 and HepSS-1, or with MPB49 (1:50 dilution), a non-HS binding phage display antibody, as a control for RB4CD12. After incubation at 4°C for 30 min, cells were washed twice with the 1× FACS buffer. Cells were then incubated in 100 μL of 1× FACS buffer containing Cy3-conjugated goat anti-Mouse IgM (3 μg/mL, for 10E4 and HepSS-1) or Cy3-conjugated anti-VSV (4 μg/mL, for RB4CD12 and MPB49) at 4°C for 30 min. Subsequently, cells were washed as above, fixed in 2% paraformaldehyde in PBS and then transferred into a 5 mL polystyrene round-bottom tube capped with a cell-strainer

cap (BD, Franklin Lakes, NJ). Antibody-bound cells were then analyzed by FACS using a FACSCalibur flow cytometer, CellQuest software (BD), and FlowJo software (Tree Star, Ashland, OR).

Preparation and structural analysis of HS

HSulf-transfected adherent cells (2×10^6 cells) cultured in OptiMEM were trypsinized for 15 min. The supernatants containing cell surface/ECM HS were collected. The HS was purified by a DEAE-Sepharose column chromatography as described (Habuchi et al. 2007). The disaccharide compositions of the HS were determined by reverse-phase ion pair chromatography with a post-column fluorescent labeling as described previously (Habuchi et al. 2007).

ELISA for Sulf activities and PI-88 inhibition

To immobilize heparin or heparan sulfate, 100 ng/mL of heparin-BSA or 1 μg/mL of heparan sulfate-BSA in PBS was added to the wells (100 μL/well) of a 96-well plate (Immulon 2HB, Dynex Laboratories). The plate was placed at 4°C overnight. The wells were washed three times with PBS containing 0.1% Tween-20 (PBS-T) and then blocked with 3% BSA (Sigma) in PBS containing 0.01% NaN_3 at RT for 2 h. The wells were washed as above and incubated with bead-bound or purified FLAG-His-tagged enzymes or concentrated MCF-7 CM in 100 μL of a reaction mixture containing 50 mM of HEPES, pH 7.5, 10 mM of $MgCl_2$ at 37°C overnight. To test for inhibitory effects of PI-88 on Sulfs, various amounts of PI-88 were incubated together with the reaction mixture. The wells were washed three times with PBS-T and then incubated with 100 μL/well of primary antibody RB4CD12 (1:750 diluted by 0.1% BSA in PBS) at RT for 1 h. The wells were washed as above and incubated with 100 μL/well of secondary rabbit anti-VSV antibody (1 μg/mL in 0.1% BSA in PBS) at RT for 45 min. Then, the wells were washed and incubated with 100 μL/well of alkali phosphatase-conjugated goat anti-rabbit IgG (0.3 μg/mL in 0.1% BSA in PBS) at RT for 45 min. The wells were washed as above and incubated with PNPP (Pierce) at RT for 5–10 min. OD 405 nm was read on a microplate reader (Bio-Rad). As previously described, we established conditions under which MCF-7 CM reduced the binding of $VEGF_{165}$ to heparin-BSA (Uchimura et al. 2006a,b). In brief, heparin-BSA coated wells were treated with MCF-7 CM in the presence of different amounts of PI-88. After the enzyme reaction, 25 μL of 25 nM human $VEGF_{165}$ was incubated on the wells for 30 min. Heparin-bound human VEGF $_{165}$ was detected with 1 μg/mL of primary goat anti-VEGF antibody, 1.2 μg/mL of biotinylated swine anti-goat antibody, and 2 μg/mL of alkali phosphatase-conjugated streptavidin. The concentration of PI-88 that inhibited the Sulf enzymatic activity by 50% (IC50) was determined using the formula: IC50 = 10^(Log [A][B] × (50 − C)/(D − C) + Log [B]), where [A] and [B] are the higher and the lower concentrations nearest to the middle of the curve, respectively, C and D are the Sulf activities at the concentration [A] and [B], respectively. Measurement of the LogIC50 value and depiction of the best-fit curve were performed using Prism software (GraphPad Software, La Jolla, CA).

Immunoblotting

The Ni-NTA agarose-bound FLAG/His-tagged Sulf proteins prepared from 0.8 mL of HEK293 transfectant CM was separated by electrophoresis on a reducing SDS–7.5% polyacrylamide gel (WAKO, Osaka, Japan) and blotted onto PVDF membrane (Millipore). The membrane was blocked with 5% skim milk/PBS-T for 1 h and then incubated overnight with an anti-FLAG tag antibody (0.2 μg/mL) in 5% skim milk/PBS-T at 4°C. The membrane was washed and incubated with horseradish peroxidase-conjugated goat anti-mouse IgG1 (0.016 μg/mL) for 1 h. Bound antibodies were visualized with SuperSignal West Pico Chemiluminescent reagent (Pierce). The H2.3 rabbit anti-HSulf-2 antibody was used to immunblot Sulf-2 in MCF-7 CM as described previously (Morimoto-Tomita et al. 2005).

Ex vivo degradation of the RB4CD12 epitope in cryostat-cut sections

Fresh brains from 12-week-old C57BL/six mice were embedded in the O.C.T. compound (Sakura Finetek, Torrance, CA) and frozen in liquid nitrogen. Cryostat-cut sections (10 μm thick) were prepared onto MAS-coated glass slides (Matsunami, Osaka, Japan), fixed in ice-cold acetone for 15 min, and then air dried for 30 min. Sections were incubated with blocking solution (3% BSA in PBS) for 15 min at RT and then pre-treated with purified HSulfs or MCF-7 CM in PBS at 37°C overnight. Sections were washed twice with PBS and then incubated with a mixture of RB4CD12 (1:100 dilution) and a rabbit anti-laminin antibody (1:100 dilution, Sigma) for 1 h at RT. Then, primary antibodies were detected with Cy3-conjugated monoclonal anti-VSV-G (4 μg/mL) and Cy2-conjugated polyclonal goat anti-rabbit IgG (3 μg/mL). Sections were mounted in FluorSaver™ Reagent (EMD Chemicals, Gibbstown, NJ). Digital images were captured by laser scanning confocal microscopy (model LSM 510, Zeiss) at the same setting for all images. The fluorescence intensities of Cy3-RB4CD12 and Cy2-laminin in stained vessels of digital images were determined semiquantitatively by Image-Pro Plus software (Media Cybernetics, Bethesda, MD).

Statistical analysis

All data are presented as means ± SD unless noted otherwise. The values were analyzed by one-way ANOVA with Tukey's (Figures 1, Figures 2, 4, and 5) or Dunnett's (6 and 7). *P*-values less than 0.05 were considered to be statistically significant.

Supplementary Data

Supplementary data for this article is available online at http://glycob.oxfordjournals.org/.

Funding

The Japanese Health and Labour Sciences Research Grant (Comprehensive Research on Aging and Health H19-001 to K.U.); the National Institutes of Health (R21 CA122025 to S.D.R., P01 AI053194 to S.D.R., R01 HL075602 to Werb-Rosen); Tobacco-Related Disease Research Program Grant (17RT-0117 to S.D.R.); and in parts by the Mochida Memorial Foundation to (K.U.); the Sumitomo Foundation (to K.U); and the Life Science Foundation of Japan (to K.U.).

Acknowledgements

We thank Durwin Tsay and Mark Singer for their technical assistance, and Zena Werb for helpful suggestions and discussion. We are grateful to Brian Creese, Vito Ferro, and Keith Dredge of Progen Pharmaceutics Ltd for kindly providing PI-88. T.H. is a Research Fellow of the Japan Foundation for Aging and Health.

Conflict of interest statement

None declared.

Abbreviations

CHO, Chinese hamster ovary; CM, conditioned medium; CS, chondroitin sulfate; ECM, extracellular matrix; ELISA, enzyme-linked immunosorbent assay; FACS, fluorescence-activated cell sorting; HEK, human embryonic kidney; HS, heparan sulfate; HSPG, heparan sulfate proteoglycan; mAb, monoclonal antibody; MFI, mean fluorescence intensity; PBS-T, 0.1% Tween 20 in PBS; scFv, single-chain variable fragment; VEGF, vascular endothelial growth factor.

References

Ai X, Do AT, Kusche-Gullberg M, Lindahl U, Lu K, Emerson CP Jr. 2006. Substrate specificity and domain functions of extracellular heparan sulfate 6-*O*-endosulfatases, QSulf1 and QSulf2. *J Biol Chem.* 281:4969–4976.

Ai X, Do AT, Lozynska O, Kusche-Gullberg M, Lindahl U, Emerson CP Jr. 2003. QSulf1 remodels the 6-*O* sulfation states of cell surface heparan sulfate proteoglycans to promote Wnt signaling. *J Cell Biol.* 162:341–351.

Ai X, Kitazawa T, Do AT, Kusche-Gullberg M, Labosky PA, Emerson CP Jr. 2007. SULF1 and SULF2 regulate heparan sulfate-mediated GDNF signaling for esophageal innervation. *Development.* 134:3327–3338.

Ambasta RK, Ai X, Emerson CP Jr. 2007. Quail Sulf1 function requires asparagine-linked glycosylation. *J Biol Chem.* 282:34492–34499.

Bernfield M, Gotte M, Park PW, Reizes O, Fitzgerald ML, Lincecum J, Zako M. 1999. Functions of cell surface heparan sulfate proteoglycans. *Annu Rev Biochem.* 68:729–777.

Bishop JR, Schuksz M, Esko JD. 2007. Heparan sulphate proteoglycans fine-tune mammalian physiology. *Nature.* 446:1030–1037.

Cosma MP, Pepe S, Annunziata I, Newbold RF, Grompe M, Parenti G, Ballabio A. 2003. The multiple sulfatase deficiency gene encodes an essential and limiting factor for the activity of sulfatases. *Cell.* 113:445–456.

Dai Y, Yang Y, MacLeod V, Yue X, Rapraeger AC, Shriver Z, Venkataraman G, Sasisekharan R, Sanderson RD. 2005. HSulf-1 and HSulf-2 are potent inhibitors of myeloma tumor growth in vivo. *J Biol Chem.* 280:40066–40073.

David G, Bai XM, Van Der Schueren B, Cassiman JJ, Van Den Berghe H. 1992. Developmental changes in heparan sulfate expression: In situ detection with mAbs. *J Cell Biol.* 119:961–975.

Dennissen MA, Jenniskens GJ, Pieffers M, Versteeg EM, Petitou M, Veerkamp JH, van Kuppevelt TH. 2002. Large, tissue-regulated domain diversity of heparan sulfates demonstrated by phage display antibodies. *J Biol Chem.* 277:10982–10986.

Dhoot GK, Gustafsson MK, Ai X, Sun W, Standiford DM, Emerson CP Jr. 2001. Regulation of Wnt signaling and embryo patterning by an extracellular sulfatase. *Science.* 293:1663–1666.

Dierks T, Schmidt B, Borissenko LV, Peng J, Preusser A, Mariappan M, von Figura K. 2003. Multiple sulfatase deficiency is caused by mutations in the gene encoding the human C(alpha)-formylglycine generating enzyme. *Cell.* 113:435–444.

Esko JD, Lindahl U. 2001. Molecular diversity of heparan sulfate. *J Clin Invest.* 108:169–173.

Esko JD, Selleck SB. 2002. Order out of chaos: Assembly of ligand binding sites in heparan sulfate. *Annu Rev Biochem.* 71:435–471.

Esko JD, Stewart TE, Taylor WH. 1985. Animal cell mutants defective in glycosaminoglycan biosynthesis. *Proc Natl Acad Sci USA.* 82:3197–3201.

Freeman SD, Moore WM, Guiral EC, Holme AD, Turnbull JE, Pownall ME. 2008. Extracellular regulation of developmental cell signaling by XtSulf1. *Dev Biol.* 320:436–445.

Frese MA, Milz F, Dick M, Lamanna WC, Dierks T. 2009. Characterization of the human sulfatase sulf1 and its high-affinity heparin/heparan sulfate interaction domain. *J Biol Chem.* 284:28033–28044.

Gallagher JT. 2001. Heparan sulfate: Growth control with a restricted sequence menu. *J Clin Invest.* 108:357–361.

Habuchi H, Habuchi O, Kimata K. 2004. Sulfation pattern in glycosaminoglycan: Does it have a code? *Glycoconj J.* 21:47–52.

Habuchi H, Nagai N, Sugaya N, Atsumi F, Stevens RL, Kimata K. 2007. Mice deficient in heparan sulfate 6-*O*-sulfotransferase-1 exhibit defective heparan sulfate biosynthesis, abnormal placentation, and late embryonic lethality. *J Biol Chem.* 282:15578–15588.

Holst CR, Bou-Reslan H, Gore BB, Wong K, Grant D, Chalasani S, Carano RA, Frantz GD, Tessier-Lavigne M, Bolon B, et al. 2007. Secreted sulfatases Sulf1 and Sulf2 have overlapping yet essential roles in mouse neonatal survival. *PLoS ONE.* 2:e575.

Iacobuzio-Donahue CA, Maitra A, Olsen M, Lowe AW, van Heek NT, Rosty C, Walter K, Sato N, Parker A, Ashfaq R, et al. 2003. Exploration of global gene expression patterns in pancreatic adenocarcinoma using cDNA microarrays. *Am J Pathol.* 162:1151–1162.

Ilan N, Elkin M, Vlodavsky I. 2006. Regulation, function and clinical significance of heparanase in cancer metastasis and angiogenesis. *Int J Biochem Cell Biol.* 38:2018–2039.

Jenniskens GJ, Hafmans T, Veerkamp JH, van Kuppevelt TH. 2002. Spatiotemporal distribution of heparan sulfate epitopes during myogenesis and synaptogenesis: A study in developing mouse intercostal muscle. *Dev Dyn.* 225:70–79.

Jenniskens GJ, Oosterhof A, Brandwijk R, Veerkamp JH, van Kuppevelt TH. 2000. Heparan sulfate heterogeneity in skeletal muscle basal lamina: Demonstration by phage display-derived antibodies. *J Neurosci.* 20:4099–4111.

Joyce JA, Freeman C, Meyer-Morse N, Parish CR, Hanahan D. 2005. A functional heparan sulfate mimetic implicates both heparanase and heparan sulfate in tumor angiogenesis and invasion in a mouse model of multistage cancer. *Oncogene.* 24:4037–4051.

Khachigian LM, Parish CR. 2004. Phosphomannopentaose sulfate (PI-88): Heparan sulfate mimetic with clinical potential in multiple vascular pathologies. *Cardiovasc Drug Rev.* 22:1–6.

Kim CW, Lee HM, Lee TH, Kang C, Kleinman HK, Gho YS. 2002. Extracellular membrane vesicles from tumor cells promote angiogenesis via sphingomyelin. *Cancer Res.* 62:6312–6317.

Kreuger J, Spillmann D, Li JP, Lindahl U. 2006. Interactions between heparan sulfate and proteins: The concept of specificity. *J Cell Biol.* 174:323–327.

Lai JP, Chien J, Strome SE, Staub J, Montoya DP, Greene EL, Smith DI, Roberts LR, Shridhar V. 2004. HSulf-1 modulates HGF-mediated tumor cell invasion and signaling in head and neck squamous carcinoma. *Oncogene.* 23:1439–1447.

Lai JP, Sandhu DS, Yu C, Han T, Moser CD, Jackson KK, Guerrero RB, Aderca I, Isomoto H, Garrity-Park MM, et al. 2008. Sulfatase 2 up-regulates glypican 3, promotes fibroblast growth factor signaling, and decreases survival in hepatocellular carcinoma. *Hepatology.* 47:1211–1222.

Lamanna WC, Baldwin RJ, Padva M, Kalus I, Ten Dam G, van Kuppevelt TH, Gallagher JT, von Figura K, Dierks T, Merry CL. 2006. Heparan sulfate 6-*O*-endosulfatases: Discrete in vivo activities and functional co-operativity. *Biochem J.* 400:63–73.

Lamanna WC, Frese MA, Balleininger M, Dierks T. 2008. Sulf loss influences *N*-, 2-*O*-, and 6-*O*-sulfation of multiple heparan sulfate proteoglycans and modulates fibroblast growth factor signaling. *J Biol Chem.* 283:27724–27735.

Li J, Kleeff J, Abiatari I, Kayed H, Giese NA, Felix K, Giese T, Buchler MW, Friess H. 2005. Enhanced levels of Hsulf-1 interfere with heparin-binding growth factor signaling in pancreatic cancer. *Mol Cancer.* 4:14.

Lin X. 2004. Functions of heparan sulfate proteoglycans in cell signaling during development. *Development.* 131:6009–6021.

Lum DH, Tan J, Rosen SD, Werb Z. 2007. Gene trap disruption of the mouse heparan sulfate 6-*O*-endosulfatase gene, Sulf2. *Mol Cell Biol.* 27:678–688.

Morimoto-Tomita M, Uchimura K, Bistrup A, Lum DH, Egeblad M, Boudreau N, Werb Z, Rosen SD. 2005. Sulf-2, a proangiogenic heparan sulfate endosulfatase, is upregulated in breast cancer. *Neoplasia.* 7:1001–1010.